Published in final edited form as:
Microcirculation. 2008 August ; 15(6): 515–529. doi:10.1080/10739680802047445.

The Cochlear Pericytes

Xiaorui Shi[*], **Weijiu Han**[*,†], **Hiroshi Yamamoto**[*], **Wenxue Tang**[‡], **Xi Lin**[‡], **Ruijuan Xiu**[§], **Dennis R. Trune**[*], and **Alfred L. Nuttall**[*,¶,″]

[*]Oregon Hearing Research Center (NRC04), Oregon Health & Science University, Portland, Oregon, USA

[†]Department of Otorhinolaryngology Head and Neck Surgery, Chinese PLA General Hospital, Beijing, China

[‡]Department of Otolaryngology, Yerkes Microarray Core, Emory University School of Medicine, Atlanta, Georgia, USA

[§]Institute of microcirculation, CAMS & PUMC, Beijing, China

[¶]Kresge Hearing Research Institute, the University of Michigan, Ann Arbor, Michigan, USA

[″]Department of Otolaryngology, Renji Hospital, Shanghai Jiao Tong University, Shanghai, China

Abstract

Objectives—Cochlear pericytes are not well characterized. The aim of this study was to further advance the characterization of cochlear pericyte location and distribution, with particular focus on pericyte-related proteins on the capillaries of the cochlear lateral wall that are functionally integral to structure, contraction, and gap junction transport.

Materials and Methods—Cochlear pericytes were identified by the immunofluorescence labeling of pericyte marker proteins, including alpha–smooth muscle actin (α-SMA), desmin, Thy-1, tropomyosin, and NG2, and by morphological identification, using fluorescence, electron, and differential interference contrast microscopy.

Results—Pericytes were predominately found in the capillary network of the cochlear lateral wall, with considerable morphological heterogeneity across different types of microvessels. For example, pericytes on the vessels of the spiral ligament (V/SL) strongly expressed a gap junction protein, connexin 40, and were positive for α-SMA, tropomyosin, and desmin. In contrast, pericytes on the vessels of the stria vascularis (V/SV) were positive for desmin, and were negative for α-SMA and tropomyosin.

Conclusions—The capillary networks of the cochlear lateral wall comprise a rich population of pericytes. These pericytes are morphologically heterogeneous, with protein expression potentially indicative of function.

Address correspondence to Xiaorui Shi, Oregon Hearing Research Center, Oregon Health & Science University, 3181 SW Sam Jackson Park Road, NRC04, Portland, OR 97239-3098, USA. shix@ohsu.edu.

Keywords

α-SMA; tropomyosin; desmin; connexin 40; NG2; cochlear pericyte

Lateral-wall blood flow in the cochlea is critical for maintaining endocochlear potential, ion transport, and endolymphatic fluid balance [29, 31, 46]. In the mature mammalian cochlea, the main terminal artery is the spiral modiolar artery, a secondary branch of the anterior inferior cerebellar artery [4, 5]. The vessels of the stria vascularis (V/SV) and the vessels of the spiral ligament (V/SL) are two major microvessel networks in the cochlea. It is known that the V/SV plays an important role in maintaining cochlear fluid homeostasis and oxygenation [28, 29, 31, 46], while the role of the V/SL is less well understood.

Pericytes are pluripotent progenitor cells surrounding blood microvessels [13]. They play a role in the regulation of blood flow, vascular permeability, maintenance of microvessel wall integrity, and angiogenesis [14, 33–35]. Pericytes are distributed in a regional and tissue-specific manner. The number of pericytes in a given area reflects specific functional features of the microvessels and is tightly coupled to metabolic demands [22, 42]. Although the critical roles played by pericytes in the retina, brain, lung, and kidney have been studied, little is known about cochlear pericytes, including their basic characterization. Two early studies by Ando [1, 44] mentioned pericyte-like cells on the capillaries of the SV of gerbils and rats, but without further elaboration. In particular, the distribution and morphology of pericytes in cochlear vascular systems is unknown. We hypothesized that the morphology and distribution of pericytes, as well as of pericyte-related proteins, were different in the capillaries of the SL and SV, given the functional differences in these two microvessel systems. Therefore, the aim of this study was to quantify pericyte numbers, determine their distribution, and investigate pericyte-related protein expression in the cochlear microvasculature of the SV and the SL. This basic characterization of pericytes is essential if the functional differences of the two lateral-wall microvessel systems are to be understood.

MATERIALS AND METHODS

Animals

Albino guinea pigs from Charles Research Laboratory (Wilmington, MA) (both sexes, age four to five weeks, weight 300–450 g) were used in this study. All animals had a positive Preyer's reflex. The procedures used in this study were reviewed and approved by the Institutional Animal Use and Care Committee of Oregon Health & Science University.

Immunohistochemistry for Pericyte-Related Proteins

Immunohistochemical methods were used to detect pericyte-related marker proteins for the identification of pericytes in the cochlear lateral wall. The guinea pigs were divided into several groups, with five animals per antibody study. After euthanasia by an overdose of ketamine hydrochloride (100 mg/kg intramuscularly [i.m.]; Abbott Laboratories, Abbott Park, Illinois, USA) and xylazine hydrochloride (2 mg/kg i.m.; Phoenix Scientific, Inc., St. Joseph, Missouri, USA), the cardiovascular system was perfused with saline, followed by a fixative perfusion of 4% paraformaldehyde. Cochleae were removed and immersed in the same fixative solution for four hours. Cochlear lateral walls from the second turn were dissected and washed in 0.02 M of phosphate-buffered saline (PBS; pH 7.4), permeabilized in 0.5% Triton X-100 (Sigma, St. Louis, MO) for one hour, then immunoblocked for one hour in a solution of 10% goat serum and 1% bovine serum albumin (BSA) in 0.02 M of PBS. The specimens of different groups were separately incubated overnight with different antibodies. Isolectin GS-IB4 (IB4) conjugated to Alexa Fluor® 488 at a concentration of 3

μg/mL (Invitrogen, Eugene, OR) was used to label vessels. Monoclonal antibodies included those for alpha–smooth muscle actin (α-SMA; Sigma, cat. no. 6198, 1:400), desmin (Epitomics, Burlingame, CA, cat. no. 1466-1, 1:400), tropomyosin (Abcam, Cambridge, MA, cat. no. ab7785, 1:400), and Thy1 (CD 90; Abcam, cat. no. ab8058-1). Rabbit polyclonal antibody for NG2 proteoglycan was from rat. The immunogen was immunoaffinity-purified NG2 chondroitin sulfate proteoglycan (Chemicon, Billerica, MA, cat. no. ab5320, 1:200). For negative control, tissues were incubated overnight with 1% BSA-PBS without a primary antibody. Specimens were washed in 1% PBS for 30 minutes after being incubated overnight with different primary antibodies and then incubated in secondary antibody, either Alexa Fluor 568 anti-rabbit IgG or Alexa Fluor 568 anti-mouse IgG (Molecular Probes, Eugene, OR, 1:100) for one hour. After washing in 0.02 M PBS for 30 minutes, the tissues were mounted and observed on a Nikon Eclipse TE 300 (Bio-Rad, Washington, DC) inverted microscope fitted with a Bio-Rad MRC 1024 confocal laser microscope system.

Immunofluorescence Measurements for α-SMA, Desmin, and Tropomysin

Protein expression was evaluated on the basis of the intensity of immunofluorescence. All images were taken on a segment (one per cochlea) of the second turn of the cochlear lateral wall within 200 μm of the segment cut ends. α-SMA expression was determined from the fluorescence intensity of 18 optical sections (six lateral-wall samples from three guinea pigs). Similarly, tropomysin expression was determined from 12 optical sections (four lateral-wall samples from two guinea pigs), and desmin expression from 40 optical sections (10 lateral wall samples from five guinea pigs). The fluorescence negative control consisted of 12 optical sections from the lateral wall of three guinea pigs. Fluorescence intensity of antibody labeling was measured in Adobe Photoshop® (San Diego, CA). For each recorded image, positive-labeled vessels were selected with a Photoshop drawing tool, and a histogram and mean value were obtained for the fluorescence intensity of the selected area. A background fluorescence intensity was read from a small window located away from the fluorescence of the vessels (background intensity had a mean value of ~50), and this background value was subtracted from the fluorescence of the vessel. The negative control was analyzed in the same way (the net fluorescence value was ~86). The resultant negative-control fluorescence was subtracted from the labeled intensities. The expression score was qualitatively defined by category. We scored expression a "−" if fluorescence was less than 86. The intensity levels between 86 and 255 (maximum) were divided in thirds. We scored 86–142 as +, 142–198 as ++, and 199–255 as +++.

Immunohistochemistry for Pericyte Gap Junction Proteins Connexin 40, Connexin 43, and Connexin 37

We examined whether gap junction proteins connexin 40 (Cx40), connexin 43 (Cx43), and connexin 37 (Cx37) were expressed between pericytes and endothelial cells. Eleven albino guinea pigs were used in this study, nine for connexin labeling and two for negative controls. The isolated and fixed second turn of cochlear lateral-wall tissues were washed in 0.02 M of PBS, permeabilized in 0.5% Triton X-100 (Sigma), and immunoblocked in 10% goat serum and 1% BSA, as mentioned above. The specimens were incubated overnight in anti-Cx40 (rabbit polyclonal antibody, cat. no. Cx40-A; Alpha Diagnostic International, San Antonio, TX) at 20 μg/mL, anti-Cx43 (rabbit polyclonal antibody, cat. no. C6219; Sigma)and diluted at 1:400 with 1% BSA-PBS and anti-Cx37 (rabbit polyclonal antibody, cat. no. cx37A11-A) at 20 μg/mL. The specimens were washed in 1% BSA-PBS for 30 minutes and incubated in Alexa Fluor 488 anti-rabbit IgG (diluted 1:100 with 1% BSA-PBS). Alexa Fluor 568 phalloidin (diluted 1:50 with 1% BSA-PBS, Molecular Probes, Eugene, Oregon, USA) was added for one hour to visualize the lateral-wall cell structure. After washing in 0.02 M of PBS for 30 minutes, the tissues were mounted on slides and

observed with the confocal laser microscope system. Negative controls were (1) tissue-incubated with 1% BSA-PBS to replace the primary antibody; (2) tissue-incubated with anti-Cx40 blocking peptide (cat. no. Cx40-P; Alpha Diagnostic International, 4 μL of antibody, 200 μL of PBS, and 10 μL of blocking peptide) overnight.

Determination of Pericyte Morphology and Distribution

We have previously shown that pericytes have high intracellular fluorescence signals for nitric oxide (NO) [40]. In this study, DAF-2DA (10 μM), a NO indicator, was used to visualize pericytes and endothelial cells. To determine pericyte morphology, after the animals were sacrificed, the cochleae were rapidly removed and transferred to a petri dish filled with a physiological solution composed of (in mM): NaCl 125, KCl 3.5, glucose 5, HEPES 10, $CaCl_2$ 1.3, and $MgCl_2$ 1.5. NaH_2PO_4 0.51 bubbled with 95% O_2 and 5% CO_2. The osmolarity of the solution was adjusted to 300 mOsm with NaCl, and the pH was adjusted to 7.4 with NaOH. The lateral wall of the cochlear second turn was dissected. The dye was added to the bath for 30 minutes and washed out with physiological solution. Tissues were then fixed with 4% paraformaldehyde for four hours prior to immunolabeling for desmin.

For the measurement of the ratio of pericytes to endothelial cells (PC/EC), the lateral wall of the cochlear second turn was labeled with DAF-2DA, as described above. Both endothelial cells and pericytes had a NO signal and could be visualized via DAF-2DA fluorescence under confocal fluorescence microscopy (Figure 1, Panel A). Pericytes (Figure 1, Panel A arrowheads) had high DAF-2DA fluorescence signals (compared with endothelial cells; Figure 1, Panel A arrows), although the mechanism for this was not clear and could thus be defined by their topographical and morphological characteristics [11, 24, 37] and colabeling with NG2 and desmin (data not shown). Pericytes were also identified by differential interference contrast (DIC) microscopy (Nikon Eclipse E 600). The numbers of endothelial cells and pericytes in both the SV and the SL were counted by tracing the contour of each DAF-2DA-labeled endothelial cell (Figure 1, Panel B green dotted lines) along the whole length of the capillaries and counting the soma of the pericytes (Figure 1, Panel B red dotted lines). Each individual endothelial cell and pericyte was counted by frequently adjusting the optical focus on different (targeted) cells along each individual vessel with moving specimen from one end to another end. We also further confirmed the numbers of pericytes and endothelial cells by counting the numbers of nuclei of pericytes and endothelial cells labeled by propidium iodide (PI, a fluorescent dye for nuclei, concentration at 1:50; Molecular Probes). The results are shown in Figure 1, Panels C and D. Endothelial cells have elongated oval- or spindle-shaped nuclei parallel to the vessel and pericytes have “bump” shaped nuclei beside the vessel walls. If two adjacent endothelial boundaries were not distinguished (fluorescence signals in the endothelial cells are not obviously lined up the shape of endothelial cells, and PI nuclei stain was uncertain), we excluded the cells from the analysis. The total number of endothelial cells and pericytes was estimated for the capillaries of the SV and the SL. For the different lateral-wall capillary areas, the sum total of pericytes was divided by the sum total of the endothelial cells to obtain the PC/EC ratio.

A pericyte soma length, as well as interpericyte distance, was measured by using a calibrated eyepiece reticule (Figure 2). DAF-2DA-labeled cochlear lateral-wall specimens were examined with fluorescence microscopy with a 40X objective. A calibrated eyepiece reticule aligned with capillary or pericyte soma allowed the measurements (Figure 2). When capillaries had significant curvature, the interpericyte distance was estimated by segmenting the curve at 10-μm intervals along the vessel center line. An average of 50 pericyte lengths was determined for each type of vessel. Distances between two pericytes were determined for each precapillary, capillary, and postcapillary region. The mean of pericyte-to-pericyte

distance on the true capillaries of the SL and the capillaries of the SV (see Figure 3, Panel B to define these capillary areas) was averaged from the randomly selected 33 vessels.

Transmission Electron Microscopy (TEM)

Dissected tissues of the second turn of the cochlear lateral wall were fixed overnight with phosphate-buffered 3% glutaraldehyde-1.5% paraformaldehyde and postfixed in 1% osmium. Tissues were dehydrated, embedded in Araldite plastic, sectioned, stained with lead citrate and uranyl acetate, and viewed in a Phillips CM100 (Fei Company, Hillsboro, OR) transmission electron microscope.

RESULTS

Cochlear Pericyte Identification

The two major systems of cochlear lateral-wall blood flow form a double layer and consist of the vessels of V/SV and the V/SL, as shown in Figure 3 (Panels A and B). The cartoon in Figure 3B illustrates Axelsson's definition of the capillary areas of the lateral wall [4]. The black vessels in the illustration within the spiral ligament were divided into three parts: precapillaries, postcapillaries, and "true" capillaries. Precapillaries and postcapillaries are defined by the absence of continuous arteriolar and venular smooth muscle. The true capillary area consists of the relatively straight vessels in the middle portion of the spiral ligament. Capillaries branch from the spiral ligament at the level precapillaries to form the true capillaries of the SV. These are highly branched and are shown in gray (Figure 3, Panel B). Pericytes were identified by multiple methods, since there are no truly specific markers for pericytes [3, 32, 36]. We used DIC microscopy, TEM, and immunofluorescence labeling of pericyte marker proteins, including NG2, desmin, Thy1, and α-SMA, combined with confocal fluorescence microscopy. Under DIC microscopy, pericytes can be morphologically recognized by their position on the outer walls of capillaries and by their characteristic "bump on a log" shape [24, 37], as shown in Panels C and D of Figure 3 (arrows). By TEM, we found pericytes in close proximity to endothelial cells. Pericytes have large nuclei and low somatic cytosole volume (Panels E and F of Figure 3). With immunofluorescence labeling, pericytes on the V/SL and the V/SV were positive for NG2, a chondroitin sulfate proteoglycan on the surface of pericytes (Figure 3, Panels G and H); desmin, a class III intermediate filament protein (Figure 3, Panels I and J); and Thy-1, a glycoprotein and pericyte cell-surface antigen (Figure 3, Panels K and L). Pericytes on the V/SL were positive for α-SMA (Figure 3, Panel M), but pericytes on the V/SV showed no immunoreactivity to α-SMA (see below).

Different Types of Pericytes in the Cochlear Lateral-Wall Microvasculature

Pericytes have higher intracellular fluorescence signals for NO than do endothelial cells of the cochlear capillary systems [40]. Using this NO indicator, combined with an antidesmin antibody, we could discern the characteristic morphology of pericytes and easily distinguish them from the endothelial cells of the capillaries, as shown in Figure 4.

We found that the shapes of pericytes differed greatly, depending on location. The majority of pericytes on true capillaries had a polygonal cell body and long, slender processes (Figure 4, Panels A–C), whereas most pericytes in the precapillary areas had prominent soma and band-like processes completely encircling the vessel, as shown in Figure 4 (Panels D–F). Most pericytes in the postcapillary venule areas had flattened cell bodies and circumferential bandlike processes completely encircling the vessel, as shown in Figure 4 (Panels G–I). The pericytes on the branch points had spindle-cell bodies and long processes distributed over two branches, as shown in Figure 4 (Panels J–L). Panels M–P in Figure 4 are further examples of pericytes at different microvessels of the cochlear lateral wall with a lower

magnification. The pericytes' long processes wrapped around capillaries were in close contact with endothelial cells.

Cochlear Pericyte Size and Distribution

Pericyte distribution and function are regional- and tissue-specific [16, 39]. Morphology and numbers are thought to reflect specific functional features of microvessels where blood flow is tightly coupled to metabolic demand [42]. In order to determine how cochlear pericytes compare with the pericytes in other vascular systems, we characterized cochlear pericyte distribution mean size, as well as mean distance between neighboring pericytes in the V/SL and V/SV. We found that the mean length of pericyte somas ranged from 9 to 11.6 μm on the different microvessel types and did not differ significantly by one-way analysis of variance (ANOVA; $P > 0.05$), but that the morphology of pericytes covered on endothelial cells varied considerably with microvessel type and location, as shown in Figure 4. The soma-to-soma distance between neighboring pericytes is given in Table 1. Pericyte soma to pericyte soma on pre- and postcapillaries ranged from 2 to 21 μm, where the distance between two neighboring pericytes on the capillaries of the SV ranged between 50 and 100 μm and on the true capillaries of the spiral ligament ranged between 50 and 87.5 μm. The distance between pericyte somas is clearly greater on the true capillaries of the SL, and the capillaries of the SV show comparable measurements in the pre- and postcapillary regions. For the true capillary of the SL, the mean distance (41 ± 23.0 μm) was not significantly different from that of the capillaries of the SV (50 ± 18.5 μm) (Table 1). The ratio of pericytes to endothelial cells on the capillaries of the V/SL was 0.76 ± 0.09 ($n_{pc} = 350$, $n_{ec} = 470$; PC, pericyte; EC, endothelial cell); for the spiral ligament, the ratio was 0.644 ± 0.08 ($n_{pc} = 99$, $n_{ec} = 155$). Density of pericytes on the two capillary systems was not statistically different ($P > 0.05$). In consideration of a potential contamination from smooth muscle, we did not statistically test the ratio of PC/EC in the pre- and postcapillary, although pre- and postcapillary in the SL are absent smooth muscle cells [4].

Distribution of Cx40 in Cochlear Pericytes

Pericytes communicate with endothelial cells via gap junctions [12]. Gap junctions are constituted by the connexin family of proteins. Gap junction proteins in pericytes have not been widely studied. It has been reported, for example, that rat retinal pericytes express Cx43 and Cx37 of the rat [26, 47]. Since different types of connexins are thought to be important for the coordination and propagation of vascular responses [21], we investigated gap junction proteins between pericytes and endothelial cells in the cochlear vasculature. With immunofluorescence techniques, we examined Cx40, Cx43, and Cx37 in the cochlear vasculature. We found that Cx40 was predominantly expressed in the pericytes and endothelial cells of the V/SL, as shown in Figure 5. In particular, Cx40 immunoreactivity was strong in pericytes on precapillaries (Figure 5, Panels A–C) and relatively weak in the true capillaries of the spiral ligament (Figure 5, Panels D–F). There was no detectable Cx40 immunoreactivity in the pericytes of the capillaries of the SV (Figure 5, Panels G–I). Cx40 immunoactivity was also strong in pericytes on postcapillaries (Figure 5, Panels J–O). Cx37 was very weakly expressed in pericytes on pre- and postcap-illaries (data not shown). No detectable immunoreactivity of Cx37 occurred in the true capillaries of the SL or capillaries of the SV (data not shown). Cx43 was not detected with our protocol. Results of control experiments without a primary antibody or with the Cx40 blocking peptide are shown in Figure 5 (Panels P–R and S–U, respectively). Alexa Fluor 568 phalloidin was used to visualize cochlear vessels and surrounding cells. Filled red circles in the drawings (Figure 5, Panels V–BB) show the locations of imaged vessels in the corresponding rows.

Contractile and Structural Proteins of Pericytes on the Cochlear Lateral-Wall Microvessels

Pericytes are morphologically, biochemically, and physiologically heterogeneous and contractility is not a ubiquitous property of pericytes [42]. To explore the potential function of cochlear pericytes in the regulation of blood flow, we investigated the expression of two major contractile proteins, α-SMA and tropomyosin, in pericytes using fluorescence immunochemical techniques. We also examined the expression of desmin, a pericyte cytoskeleton protein that plays an important role in the maintenance of vascular-wall integrity [20, 38].

α-SMA—α-SMA immunofluorescence varied across different areas of the cochlear lateral wall. As we show in Figure 6, α-SMA-positive labeling was observed in regions of the V/SL. By contrast, no detectable α-SMA immunolabeling was observed on the V/SV (Figure 6, Panels G–I). This suggests that pericytes on SL vessels may have contractile functions, while those on the SV may not. IB4 was used to label the vessels.

Tropomyosin—Positive tropomyosin immunolabeling was also found on the pericytes of the V/SL (Figure 7, Panel A), but little was seen on the V/SV (shown in Figure 7, Panel B).

Desmin—With immunofluorescence techniques, we found that pericytes on both the V/SL and the V/SV were positive for desmin (Figure 8, Panels A and B), in particular, pericytes' long processes labeled for desmin filament protein. The vessels were labeled by IB4.

Heterogeneity of Microvascular Pericytes for Contractile Proteins in the V/SL and the V/SV—The average of immunofluorescence intensity was used to determine the relative preponderance of α-SMA, tropomysin, and desmin expression in pre-, true-, and postcapillary pericytes (see Methods). We found heterogeneity of expression, shown schematically in Figure 9. In general, all pericytes on the V/SL were positive for α-SMA, tropomyosin and desmin. The relative intensity of the labeling for α-SMA, tropomyosin, and desmin in pre- (arteriole side) and postcapillary (venule side) pericytes was high in comparison to the expression in pericytes of the true capillaries of the SL. Pericytes on the capillaries of the SV were devoid of both α-SMA and tropomyosin labeling but positive for desmin.

DISCUSSION

Pericytes are morphologically heterogeneous from organ to organ [42]. Although much is known about pericytes in general, little is known about cochlear pericytes. In this study, we identified and characterized the morphology of cochlear pericytes. Since there are no specific markers for pericytes, we identified them by using combinations of marker proteins with fluorescence microscopy, as well as on the basis of morphological characteristics, an approach that has published validity [3, 11, 24, 37]. The ratio of pericytes to endothelial cells on the regions of the capillaries of the SV and the SL defined by Axelsson [4] were between 1:1 and 1:2, which is a relatively high ratio compared to the ratio in most other organs; for example, the ratio of pericytes to endothelial cells in the brain is 1:5, in lung 1:10, and in skeletal muscle 1:100 [16, 39]. An exception is the retina, where the ratio is 1:1 [39]. The ratio of pericytes to endothelial cells on the regions of pre- and postcapillaries was not calculated in this study, as there possibly was a gradual transition between pericytes and smooth muscle cells in both terminal arterioles and venules [3, 11].

In general, the characteristics of pericytes are regional- and tissue-specific and reflect the specific functional features of the microvessels, including the coupling to metabolic demand. For example, pericytes in the brain play roles in the central nervous system, including roles

in microvascular contractility, regulation of endothelial cell activity, and maintenance of function of the blood-brain barrier [25, 36, 45]. Certain pericytes in the kidney glomerulus form high-density tufts, which are continuous treelike cores around the capillary loops. The structure of these tufts serves to meet regional blood-flow demand [19]. Also, retinal microvasculature does not contain sphincter muscle, and pericytes play a role in modulating retinal perfusion [35].

The vulnerability of lateral-wall and hair cells to the hypoxia requires an adequate cochlear blood flow to be maintained. This is especially true with exposure to long-duration sounds. The high density of pericytes in the microvasculature of the cochlea may be related to functional and metabolic needs in the innerear. For example, cochlear microvessels show a strong intrinsic regulation of cochlear blood flow [8, 9] despite their lack of cholinergic innervation. Pericytes may be required to control local blood flow and buttress vessel stability in the cochlear vascular system, as has been reported to be the case in the brain [27, 30, 33] and retina [7, 34]. However, our experimental data were too preliminary to permit us to draw conclusions regarding physiological function.

Pericytes located on different types of microvessels show structural differences. In general, pre- and postcapillary bed pericytes exhibit more contact with the endothelium, with extensive short processes, and the distance between neighboring pericyte soma is closer (approximately 2–25 μm). Pericytes on true capillaries of the spiral ligament and the capillaries of the SV have longer processes (up to 100 μm in length) and pass and make contact with several endothelial cells along the long axis of the vessel, but have fewer short processes encircling the vessel walls. These differences in distribution and structure suggest the pericytes may have different functions relating to contractile activity, mechanical support, and intercellular communication.

Pericytes on the V/SL are positive for two contractile proteins: α-SMA and tropomyosin. In addition, pericytes on pre- and postcapillary beds had greater α-SMA and tropomyosin immunoreactivity than capillaries of the spiral ligament. In contrast, pericytes on the V/SV were devoid of α-SMA and tropomyosin. These results are in agreement with an early report finding differential expression of contractile proteins in the capillaries of the SV and SL [17]. Both α-SMA and tropomyosin are essential for pericyte contraction and relaxation [14]. Pericyte contractility in the SV may be lacking or greatly attenuated.

Additionally, pericytes on the V/SV and the V/SL in the cochlea are positive for desmin, an intermediate filament protein. Desmin has a significant role in the structural and mechanical integrity of the contractile apparatus in muscle tissue [43]. Mice lacking desmin postnatally develop a dilated cardiomyopathy [6, 20]. The physiological role of desmin in the two vessel systems of the cochlea is not clear at this moment. Capillaries of the SV are lacking in collagen and extracellular matrix, except for the basal lamina around the capillaries [2]. Pericytes may be functioning as a mechanical part of the vessel wall. Desmin fibers are also important for the transmission of mechanical loads and possibly for the initiation of signal-transduction cascades via mechanical force interconnections to the organelles [38]. Vascular perfusion requires cellular coordination [10, 15], and the cochlear pericytes' long processes, wrapped around capillaries in close contact with endothelial cells, may set the stage for signal integration, as has been reported in brain pericytes [33]. Peppiatt [33] found that the long cytoplasmic processes of pericytes in the brain can integrate signals along the length of the vessel.

Pericytes can communicate with endothelial cells by direct physical contact and through paracrine-signaling pathways [18]. The signals may convey information on the metabolic state of the SV and serve to regulate blood flow, which are similar to roles that have been

found for pericytes in other organs [13, 25, 33–35]. Cochlear pericytes and endothelial cells have been shown to communicate via gap junctions [2]. Gap junctions are membrane channels that permit the direct exchange of inorganic ions, sugars, amino acids, nucleotides, and signaling molecules smaller than 1,000 Da [23]. The composition of gap junctions between the pericytes and endothelium has not been widely studied. A few studies have found proteins, such as Cx43 and Cx37, in pericytes and in endothelial cells of retina and brain microvasculature [26, 41]. In the cochlear lateral wall, we found that Cx40 (but not Cx37 or Cx43) was abundantly expressed in endothelial cells and pericytes on the vessels of the spiral ligament, but not on the vessels of the SV. Retinal and brain pericytes express both Cx37 and Cx43. It has been suggested these variations in connexin have important consequences for the coordination and propagation of vascular signals and responses [21]. The heterogeneity of Cx40 expression in the cochlea may be of physiological significance, suggesting differences in metabolic information processing that warrant further investigation.

CONCLUSIONS

Microvessels in the cochlear lateral wall are densely populated with pericytes. There are morphological differences between the pericytes on the V/SL and the V/SV. An array of pericyte-related proteins, including α-SMA, desmin, and tropomyosin, are found in the pericytes on the V/SL. However, pericytes on the V/SV are positive only for desmin. No detectable α-SMA or tropomyosin was found in the pericytes on the V/SV. Pericytes on the V/SL also strongly express Cx40. The data support the view that pericytes on the vessels of the SL have a role in the control of local blood flow, whereas pericytes on the vessels of the SV may only serve a structural role related to microvessel-wall integrity [30].

Acknowledgments

The authors thank Professor Donald G. Puro, MD, PhD (at the Department of Ophthalmology and Visual Science Department of Physiology, Kellogg Eye Center, Ann Arbor, MI) and Dr. Brian Duling, PhD (at the Department of Molecular Physics and Biological Physics, University of Virginia, Charlottesville, VI) for their helpful comments on an earlier draft of this manuscript. The authors also thank Jackie De-Gahne for assistance with the transmission electron microscope technique.

This research was supported by NIH/NIDCD Grants R03 DC 008888-02 and R01 DC 00105, DC005983.

REFERENCES

1. Ando M, Kakigi A, Takeuchi K. Elongated pericyte-like cells connect discrete capillaries in the cochlear stria vascularis of gerbils and rat. Cell Tissue Res. 1999; 296:673–676. [PubMed: 10370153]
2. Ando M, Takeuchi S. Postnatal vascular development in the lateral wall of the cochlear duct of gerbils: quantitative analysis by electron microscopy and confocal laser microscopy. Hear Res. 1998; 123(1–2):148–156. [PubMed: 9745963]
3. Armulik A, Abramsson A, Betsholtz C. En-dothelial/pericyte interactions. Circ Res. 2005; 97:512–523. [PubMed: 16166562]
4. Axelsson A. The vascular anatomy of the cochlea in the guinea pig and in man. Acta Otolaryn-gol (Stockh). 1968; (Suppl):243. 3+.
5. Axelsson A, Vertes D. Vascular histology of the guinea pig cochlea. Acta Otolaryngol (Stockh). 1978; 85:198–212. [PubMed: 345736]
6. Bar H, Mucke N, Ringler P, Muller SA, Kreplak L, Katus HA, Aebi U, Herrmann H. Impact of disease mutations on the desmin filament assembly process. J Mol Biol. 2006; 360:1031–1042. [PubMed: 16828798]

7. Benjamin L, Hemo I, Keshet E. A plasticity window for blood vessel remodelling is defined by pericyte coverage of the preformed endothelial network and is regulated by PDGF-B and VEGF. Development. 1998; 125:1591–1598. [PubMed: 9521897]
8. Brechtelsbauer PB, Ren T-Y, Miller JM, Nuttall AL. Autoregulation of cochlear blood flow in the hydropic guinea pig. Hearing Res. 1995; 89:130–136.
9. Brown JN, Nuttall AL. Autoregulation of cochlear blood flow in guinea pigs. Am J Physiol. 1994; 266:H458–H467. [PubMed: 8141346]
10. de Witt C, Hoepfl B, Wolfle SE. Endothelial mediators and communication through vascular gap junctions. Biol Chem. 2006; 387:3–9. [PubMed: 16497158]
11. Diazflores L, Gutierrez R, Varela H, Rancel N, Valladares F. Microvascular pericytes: a review of their morphological and functional-characteristics. Histol Histopathol. 1991; 6:269–286. [PubMed: 1802127]
12. Donoghue L, Tyburski JG, Steffes CP, Wilson RF. Vascular endothelial growth factor modulates contractile response in microvascular lung pericytes. Am J Surg. 2006; 191:349–352. [PubMed: 16490545]
13. Dore-Duffy P, Katychev A, Wang X, Van Buren E. CNS microvascular pericytes exhibit multi-potential stem cell activity. J Cereb Blood Flow Metab. 2006; 26:613–624. [PubMed: 16421511]
14. Edelman DA, Jiang Y, Tyburski J, Wilson RF, Steffes C. Pericytes and their role in microvasculature homeostasis. J Surg Res. 2006; 135:305–311. [PubMed: 16930620]
15. Figueroa XF, Alvina K, Martinez AD, Garces G, Rosemblatt M, Boric MP, Saez JC. Histamine reduces gap junctional communication of human tonsil high endothelial cells in culture. Microvasc Res. 2004; 68:247–257. [PubMed: 15501244]
16. Frank R, Dutta S, Mancini M. Pericyte coverage is greater in the retinal than in the cerebral capillaries of the rat. Invest Ophthalmol Vis Sci. 1987; 28:1086–1091. [PubMed: 3596989]
17. Franz P, Helmreich M, Stach M, Franz-Italon C, Bock P. Distribution of actin and myosin in the cochlear microvascular bed. Acta Oto-Laryngol. 2004; 124:481–485.
18. Fujimoto K. Pericyte-endothelial gap junctions in developing rat cerebral capillaries: a fine structural study. Anat Rec. 1995; 242:562–565. [PubMed: 7486026]
19. Gerhardt H, Christer B. Endothelial-pericyte interactions in angiogenesis. Cell Tissue Res. 2003; 314:15–23. [PubMed: 12883993]
20. Goldfarb LG, Vicart P, Goebel HH, Dalakas MC. Desmin myopathy. Brain. 2004; 127:723–734. [PubMed: 14724127]
21. Hill JK, Gillespie PG. Differential regulation of pH in the soma and bundle of hair cells. Biophys J. 2002; 82:567A.
22. Hirschi KK, D'Amore PA. Pericytes in the microvasculature. Cardiovasc Res. 1996; 32:687–698. [PubMed: 8915187]
23. Inai T, Mancuso MR, McDonald DM, Kobayashi J, Nakamura K, Shibata Y. Shear-stress-induced upregulation of connexin 43 expression in endothelial cells on upstream surfaces of rat cardiac valves. His-tochem Cell Biol. 2004; 122:477–483.
24. Kuwabara T, Cogan D. Studies of retinal vascular patterns. Arch Ophthalmol. 1960; 64:904–911. [PubMed: 13755464]
25. Lai CH, Kuo KH. The critical component to establish *in vitro* BBB model: pericyte. Brain Res Mol Brain Res. 2005; 50:258–265.
26. Li AF, Sato T, Haimovici R, Okamoto T, Roy S. High glucose alters connexin 43 expression and gap junction intercellular communication activity in retinal pericytes. Invest Ophthalmol Vis Sci. 2003; 44:5376–5382. [PubMed: 14638741]
27. Lindahl P, Johansson BR, Leveen P, Betsholtz C. Pericyte Loss and microaneurysm formation in PDGF-B-deficient mice. Science. 1997; 277:242–245. [PubMed: 9211853]
28. Mazurek B, Haupt H, Georgiewa P, Klapp BF, Reisshauer A. A model of peripherally developing hearing loss and tinnitus based on the role of hypoxia and ischemia. Med Hypoth. 2006; 67:892–899.
29. Miller JM, Ren TY, Nuttall AL. Studies of inner ear blood flow in animals and human beings. Oto-laryngol Head Neck Surg. 1995; 112:101–113.

30. Nakagawa S, Deli MA, Nakao S, Honda M, Hayashi K, Nakaoke R, Kataoka Y, Niwa M. Pericytes from brain microvessels strengthen the barrier integrity in primary cultures of rat brain endothelial cells. Cell Mol Neurobiol. 2007; 27:687–694. [PubMed: 17823866]

31. Nakashima T, Naganawa S, Sone M, Tominaga M, Hayashi H, Yamamoto H, Liu X, Nuttall AL. Disorders of cochlear blood flow. Brain Res Rev. 2003; 43:17–28. [PubMed: 14499459]

32. Nehls V, Drenchhahn D. The versatility of microvascular pericytes: from mesenchyme to smooth muscle? Histochem Cell Biol. 1993; 99:1–12.

33. Peppiatt CM, Howarth C, Mobbs P, Attwell D. Bidirectional control of CNS capillary diameter by pericytes. Nature. 2006; 443:700–704. Epub, 2006 Oct 2001. [PubMed: 17036005]

34. Puro DG. Physiology and pathobiology of the pericyte-containing retinal microvascular: new developments. Microcirculation. 2007; 14:1–10. [PubMed: 17365657]

35. Quignard JF, Harley EA, Duhault J, Vanhoutte PM, Feltou M. K^+ channels in cultured bovine retinal pericytes: effects of beta-adrenergic stimulation. J Cardiovasc Pharmacol. 2003; 42:379–388. [PubMed: 12960683]

36. Rucker HK, Wynder HJ, Thomas WE. Cellular mechanisms of CNS pericytes. Brain Res Bull. 2000; 51:363–369. [PubMed: 10715555]

37. Sakagami K, Wu DM, Puro DG. Physiology of rat retinal pericytes: modulation of ion channel activity by serum-derived molecules. J Physiol (Lond). 1999; 521:637–650. [PubMed: 10601495]

38. Shah SB, Davis J, Weisleder N, Kostavassili I, McCulloch AD, Ralston E, Capetanaki Y, Lieber RL. Structural and functional roles of desmin in mouse skeletal muscle during passive deformation. Biophys J. 2004; 86:2993–3008. [PubMed: 15111414]

39. Shepro D, Morel NM. Pericyte physiology. FASEB. 1993; 7:1031–1038.

40. Shi XR, Ren TY, Nuttall AL. Nitric oxide distribution and production in the guinea pig cochlea. Hear Res. 2001; 153:23–31. [PubMed: 11223294]

41. Simard M, Arcuino G, Takano T, Liu QS, Nedergaard M. Signaling at the gliovascular interface. J Neurosci. 2003; 23:9254–9262. [PubMed: 14534260]

42. Sims DE. Diversity within pericytes. Clin Ex-per Pharmacol Physiol. 2000; 27:842–846.

43. Stewart M. Intermediate filament structure and assembly. Curr Opin Cell Biol. 1993; 5:3–11. [PubMed: 8448027]

44. Takeuchi S, Ando M. Dye-coupling of melanocytes with endothelial cells and pericytes in the cochlea of gerbils. Cell Tissue Res. 1998; 293:271–275. [PubMed: 9662649]

45. Thomas WE. Brain macrophages: on the role of pericytes and perivascular cells. Brain Res. 1999; 31:42–57.

46. Wangemann P. Cochlear blood flow regulation. Adv Otorhinolaryngol. 2002; 59:51–57. [PubMed: 11885661]

47. Zhang Q, Cao C, Mangano M, Zhang Z, Silldorff EP, Lee-Kwon W, Payne K, Pallone TL. Descending vasa recta endothelium is an electrical syncytium. Am J Physiol Regul Integr Comp Physiol. 2006; 291:R1688–R1699. [PubMed: 16840652]

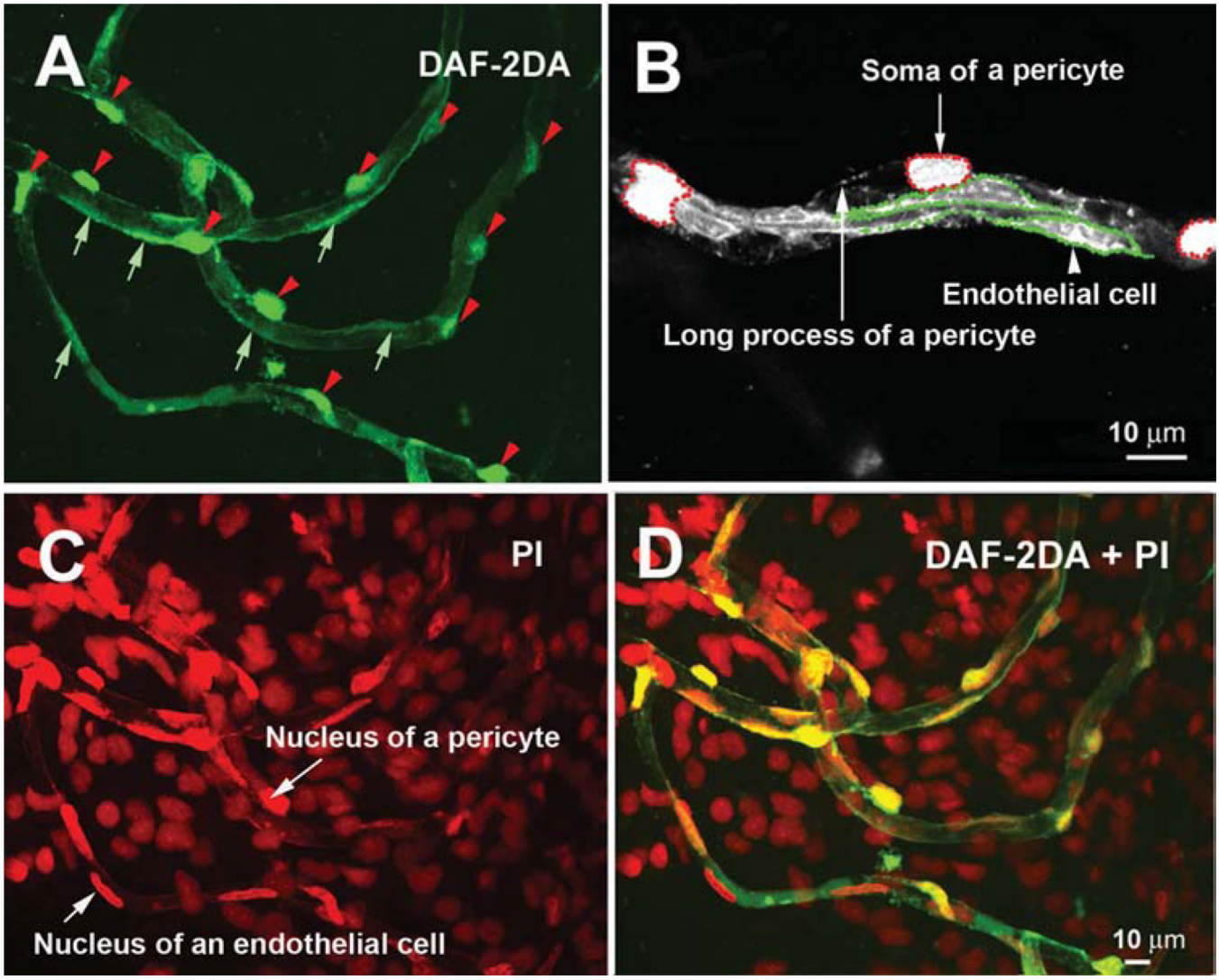

Figure 1.

An illustration of the measurement of the ratio of pericytes to endothelial cells. Panel A shows that both endothelial cells and pericytes can be visualized by the DAF-2DA label (the red arrow heads point to the somas of pericytes; the short green arrows point out the endothelial cells). Panel B, an image at higher magnification, shows that both pericyte somas (defined by the red dotted lines) and endothelial cells (defined by the green dotted lines) can be recognized by DAF-2DA fluorescence and by location along the vessel wall. Panel C cell nuclei in the whole-mount lateral wall are labeled with propidium iodide (a short arrow points at a nucleus of an endothelial cell; a long arrow points at a nucleus of pericyte). Panel D is a merged image from Panels A and C.

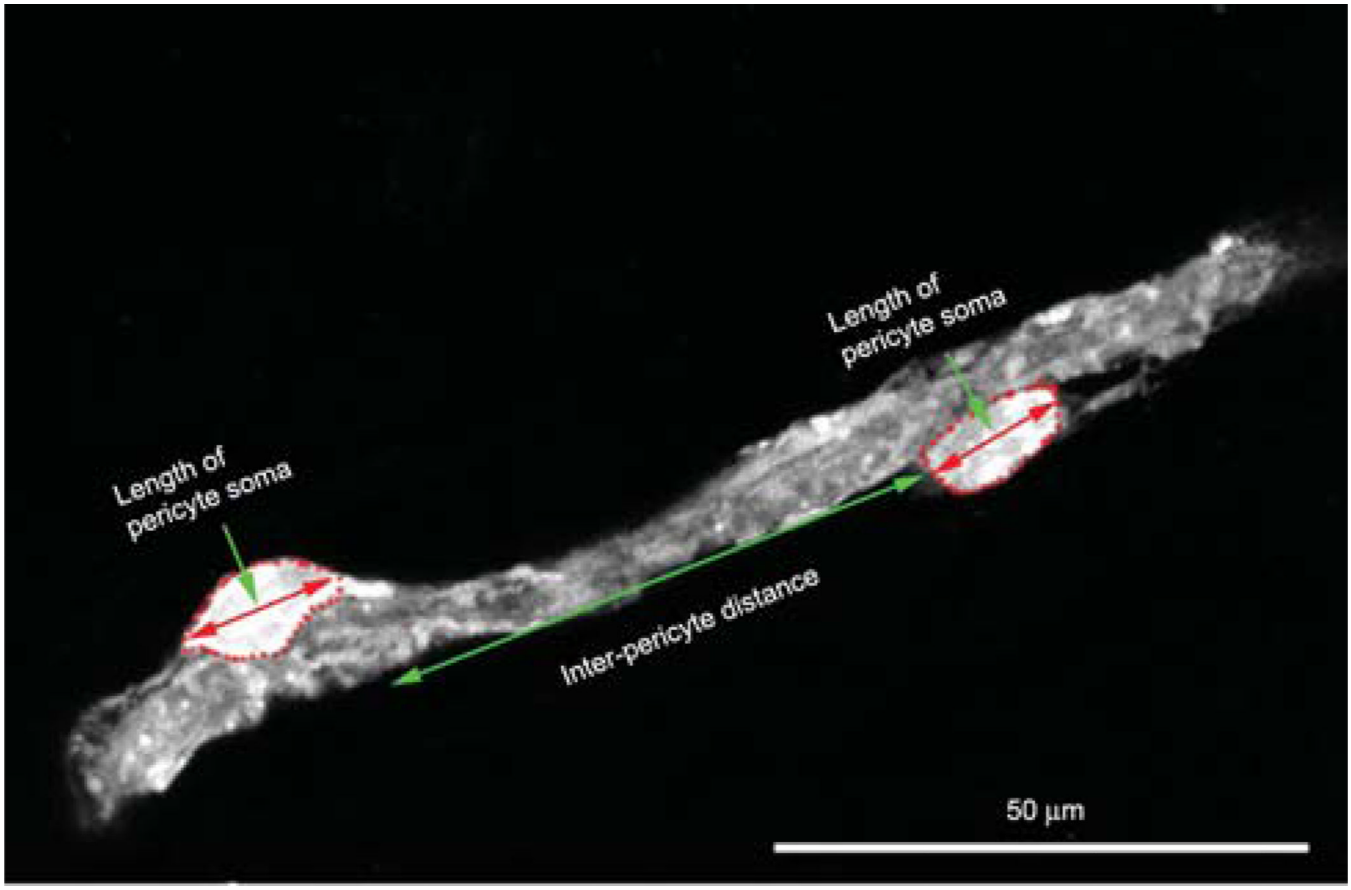

Figure 2.
An illustration of the measurement of pericyte soma size (short double-ended arrow) and interpericyte distance (long double-ended arrow).

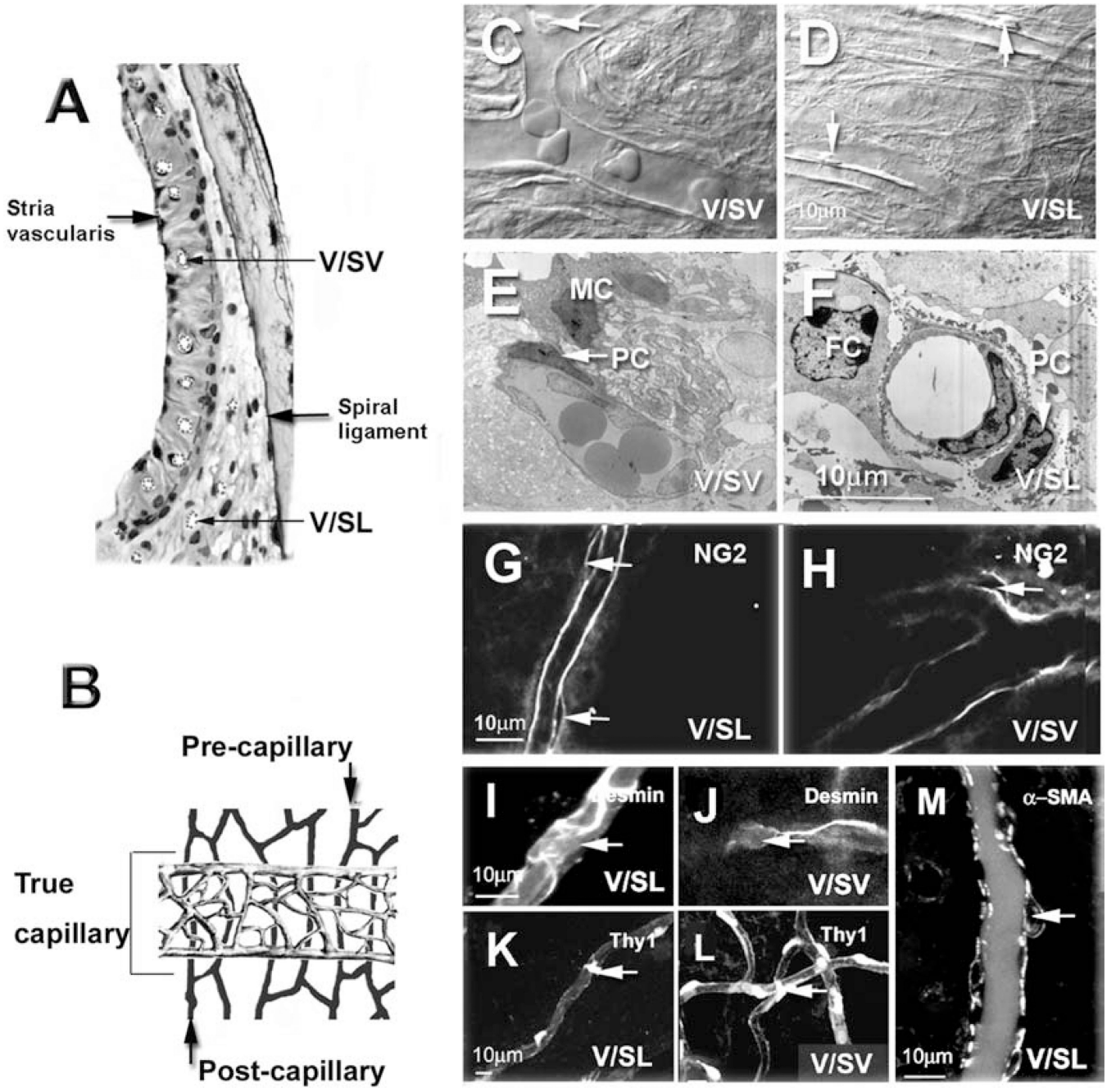

Figure 3.

Pericyte identification with differential interference contrast (DIC), transendothelial migration (TEM), and pericyte marker proteins. Panel A shows a bright-field micrograph of a cross-section of the cochlear lateral wall showing locations of the capillary networks of the stria vascularis and the spiral ligament. The vessels are emphasized by dotted lines. Panel B shows a schematic drawing of the anatomy of the cochlear lateral wall of two main capillary networks: V/SL, shown in black, and the vessels V/SV, shown in grey. V/SLs are categorized as precapillary, true capillary, and postcapillary (see text). Panels C and D show examples of pericytes present on the vessel wall of the spiral ligament (Panel C) and on the stria vascularis (Panel D) under DIC microscopy. Pericytes are identified by their

characteristic “bump on a log” shape (the arrows point to pericyte nuclei). Panels E and F show that pericytes have a large nuclei-to-somatic-cytosol ratio and are closely associated with endothelial cells under TEM microscopy (the arrows point to pericyte nuclei: FC, fibrocyte; PC, pericyte; MC, marginal cell). Panels G and H show pericytes labeled for NG2, a pericyte marker protein. Panel G shows two pericytes on the V/SL with NG2 (a confocal single image, the arrows point at pericytes). Panel H shows a pericyte on the V/SV with NG2 (a confocal single image, the arrow points at the pericyte). Panels I and J show pericytes labeled for desmin, a pericyte marker protein. Panel I shows a pericyte on the V/SL with a desmin label (a confocal projection image from 12 optical sections; interval: 1 μm, the arrow points at the pericyte). Panel J shows a pericyte on the V/SV with a desmin label (confocal projection images from 10 optical sections; interval: 1 μm, the arrow points at pericyte). Panels K and L show pericytes labeled with the second pericyte marker protein, Thy1. Panel K shows a pericyte on the V/SL (confocal projection images from 11 optical sections, interval: 1 μm, the arrow points at the pericyte). Panel L shows a pericyte on the V/SV (confocal projection images from 12 optical sections; interval: 1 μm, the arrow points at the pericyte). Panel K, a single confocal optical section, showing pericytes on a vessel of SL labeled using another pericyte marker protein, alpha–smooth muscle actin (α-SMA). Pericytes on the vessels of SV did not label for α-SMA (see Figure 6).

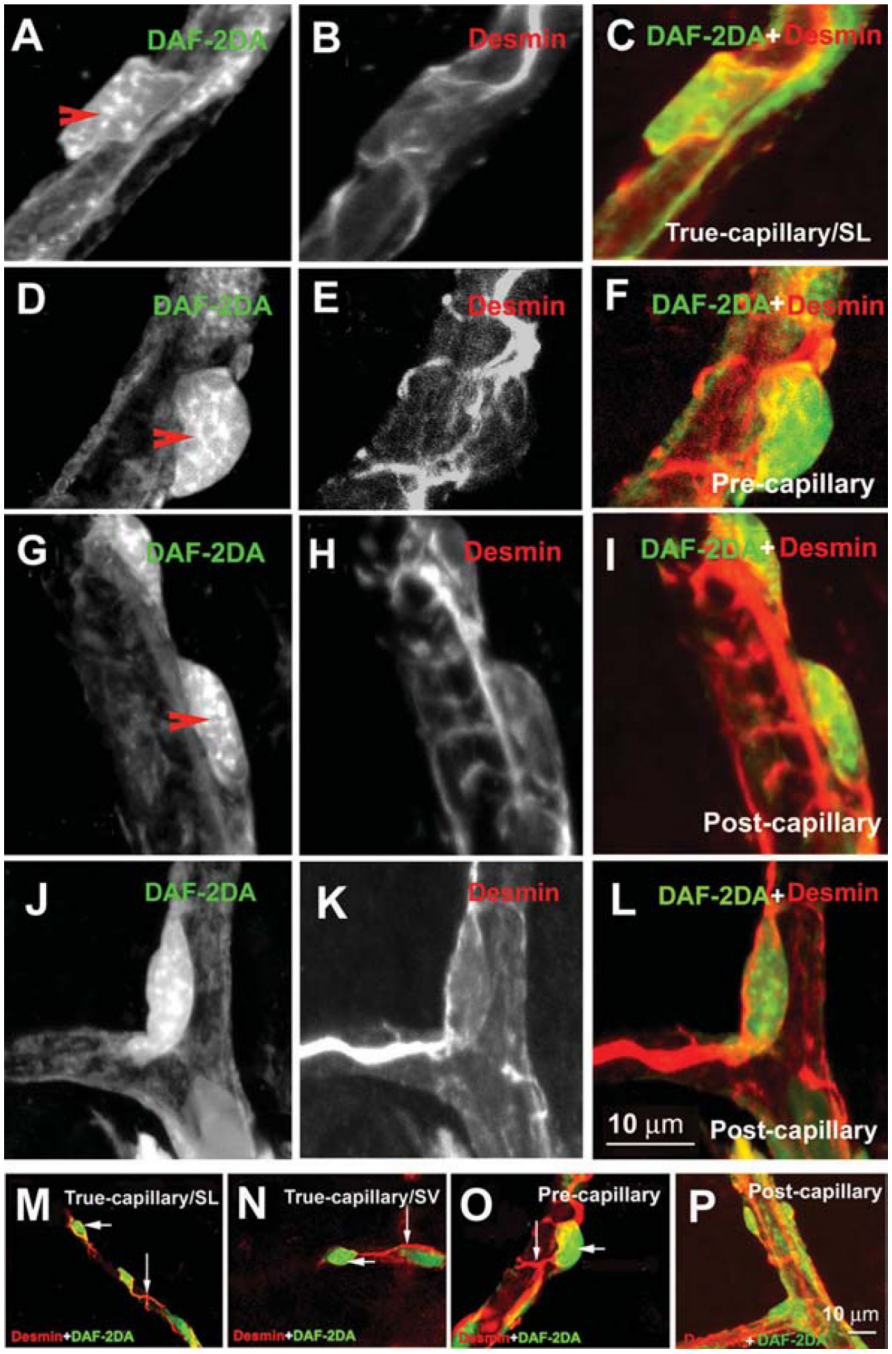

Figure 4.

Different shapes of pericytes on different cochlear microvessels. The pericytes were double-labeled with a pericyte marker protein: desmin (red), combined with fluorescence DAF-2DA for intracellular nitric oxide (green). Panels A–C show the morphology of pericyte on a true capillary. The pericyte has a polygonal-shaped cell body (Panel A, 10 sections; interval: 1 μm) and relatively few long longitudinal processes, with short, fine circumferential processes (Panel B, 10 sections; interval: 1 μm). Panel C shows a merged image from Panels A and B. Panels D–F show the morphology of pericyte on a precapillary. The pericyte has "bump shaped" soma (Panel D, 11 sections; interval: 1 μm) and relatively large processes that encircled the capillary (Panel E, 10 sections; interval: 1 μm). Panel F shows a merged

image from Panels D and E. Panels G–I show the morphology of pericytes on a postcapillary. They have a flattened cell body (Panel G, 11 sections; interval: 1 μm) and short processes encircling the vessel (Panel H, 11 sections; interval: 1 μm). Panel I shows a merged image from Panels G and H. Panels J–L show the morphology of a pericyte on a branch point of the postcapillary. The pericyte has a spindle-shaped cell body (Panel J, 10 sections; interval: 1 μm) and long processes distributed over two branches (Panel K, 10 sections; interval: 1 μm). Panel L shows a merged image from Panels J and K. Panels M–P are additional examples of pericytes' morphological variation. Panels M and N show pericytes on true capillaries of the spiral ligament (Panel M, 11 sections; interval: 1 μm) and the stria vascularis (Panel N, 9 sections; interval: 1 μm). Panel O shows pericytes on a precapillary (10 sections; interval: 1 μm). Panel P shows pericytes on a postcapillary (8 sections; interval: 1 μm).

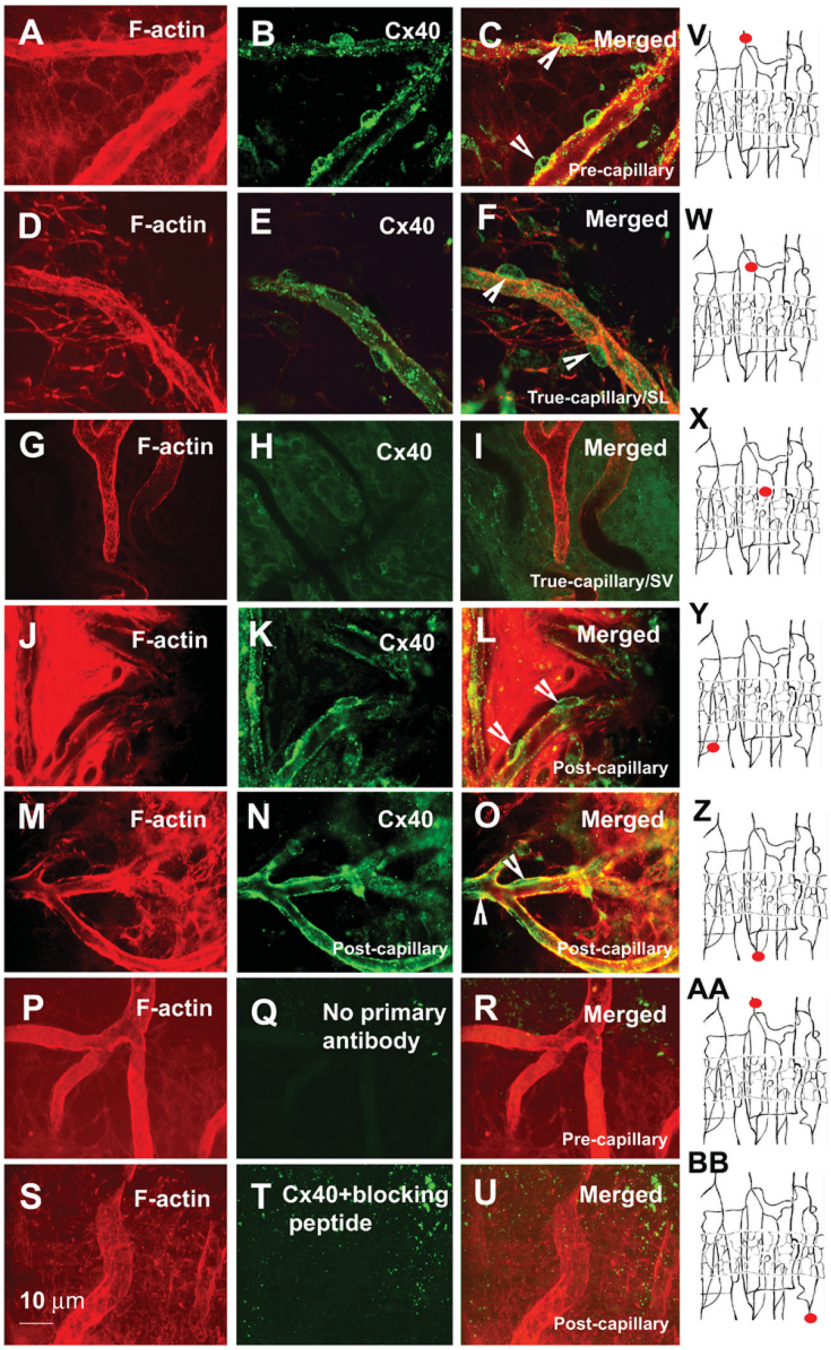

Figure 5.

Confocal immunofluorescence images of Cx40 expression in different pericytes and microvessels. Panel A, a confocal projection image from three optical sections (interval: 2 μm) shows lateral-wall tissues, including precapillaries labeled by Alexa Fluor® 568 phalloidin. Panel B shows Cx40 expression in the pericytes on these precapillaries. Panel C, a merged image from Panels A and B (the arrow heads point at the pericyte). Panel D, a confocal projection image from 13 optical sections (interval: 1.5 μm) shows a true capillary of spiral ligament (SL). Panel E shows Cx40 expression in the pericytes on this capillary. Panel F shows a merged image from Panels C and D (the arrow heads point at the pericyte). Panel G, a confocal single image, shows a capillary of the stria vascularis (SV). Panel H

shows no detectable Cx40 expression in the pericytes on these capillaries. Panel I, a merged image from Panels G and K. Panel J, a confocal single optical image, shows a postcapillary of SL. Panel K shows Cx40 expression in the pericytes of these postcapillaries. Panel L, a merged image from Panels J and K (arrow heads point at pericyte). Panel M, a confocal single optical image, shows the postcapillaries of the SL. Panel N shows Cx40 expression in the pericytes on these postcapillaries. Panel O, a merged image from Panels M and N. Panels P and S, confocal single optical images, show postcapillaries of the spiral ligament. Panels Q and T show no immunoreactivity for Cx40 in the pericytes on the postcapillaries when tissues were incubated with either a second antibody alone (Panel Q, confocal projection image from eight optical sections; interval: 2.0 μm) or an anti-Cx40 antibody-blocking peptide (Panel T, confocal projection image from 13 optical sections). Panels R and U, merged images from either Panels P and Q or Panels S and T. Panels V–BB are drawings, showing the locations of imaged vessels (small filled red circles) in the corresponding rows.

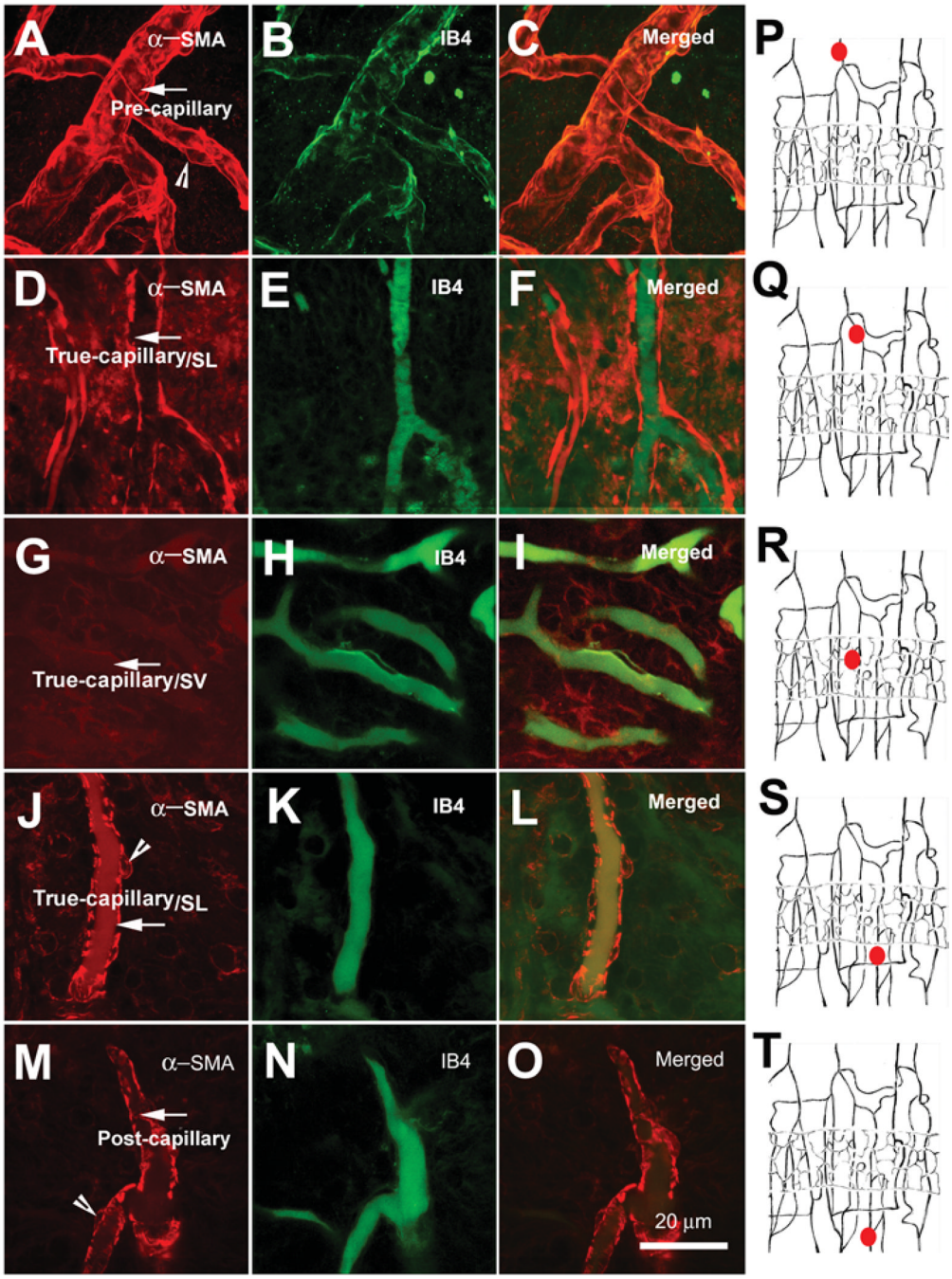

Figure 6.

Confocal single optical section images of the immunolabeled alpha–smooth muscle actin (α-SMA) (red) in whole mounts of lateral-wall vessels labeled with isolectin, IB4 (green). Panels A, D, G, J, and M show α-SMA distribution (red) in the different areas of the vessels of the stria vascularis (V/SV) and the spiral ligament (V/SL) (the arrows point at the vessels; the arrow heads point at the pericytes). Panels B, E, H, K, and N show the vascular structure in the different locations of the cochlear lateral wall revealed with isolectin, an IB4 label. Panels C, F, I, L, and O show merged images of the left and middle of columns. Panels P–T, drawings, show the locations of imaged vessels (small filled red circles) in the

corresponding rows. The α-SMA was only detected in the V/SL system, not in the V/SV (Panel G).

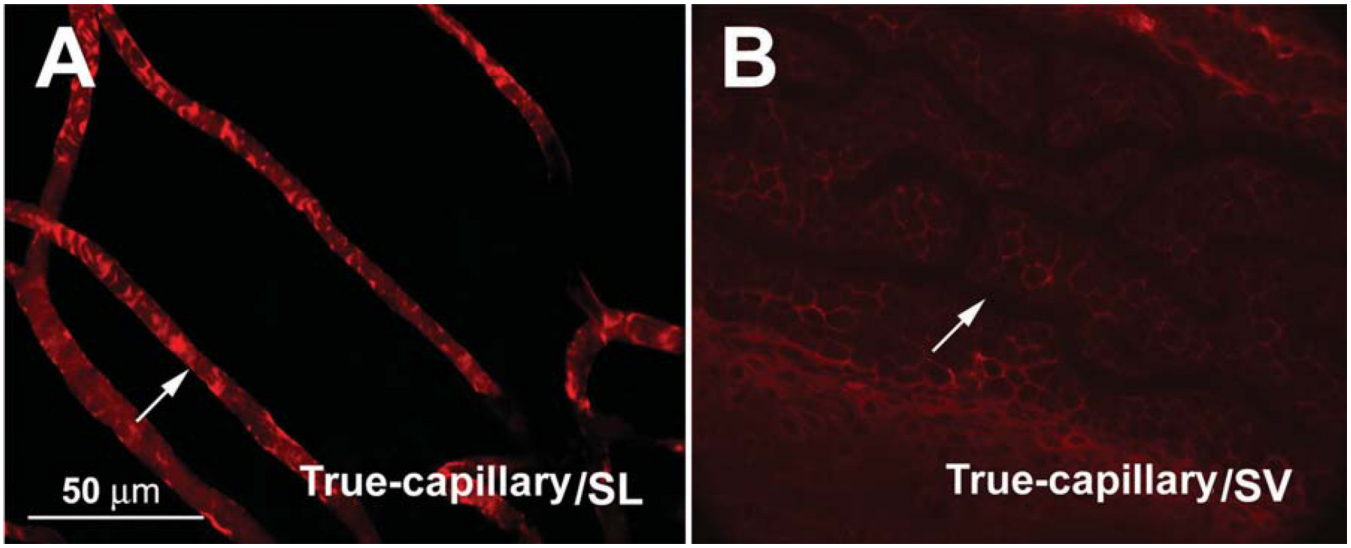

Figure 7.
Confocal projection images of the immunolabeled tropomyosin (red) in the vessels of the stria vascularis (V/SV) and spiral ligament (V/SL) of the adult guinea pig. Panel A shows positive immunoreactivity for tropomyosin in the capillaries of the SL (eight sections; interval: 2 μm). Panel B shows no detectable tropomyosin immunoreactivity in the capillaries of the SV (13 sections; interval: 1 μm).

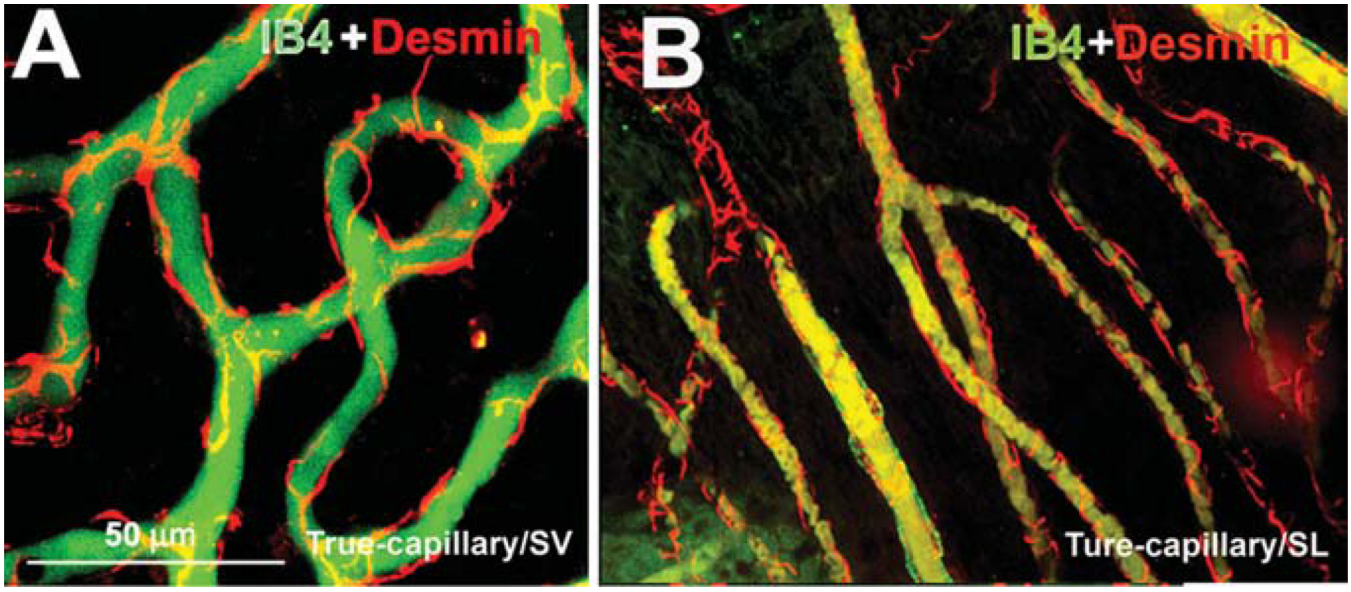

Figure 8.

Confocal projection images of immunolabeled desmin pericytes on capillaries labeled with isolectin (IB4) from the cochlear lateral wall of an adult guinea pig. Panel A (16 sections; interval: 1 μm) shows desmin distribution along the capillary walls of the spiral ligament (SL) (red); IB4 labeling (green) shows the structure of the capillaries of the SL. Panel B (19 sections; interval: 1 μm) shows desmin filaments distributed along the capillary walls of the stria vascularis (SV) (red); IB4 labeling (green) shows the structure of the capillaries of the SV.

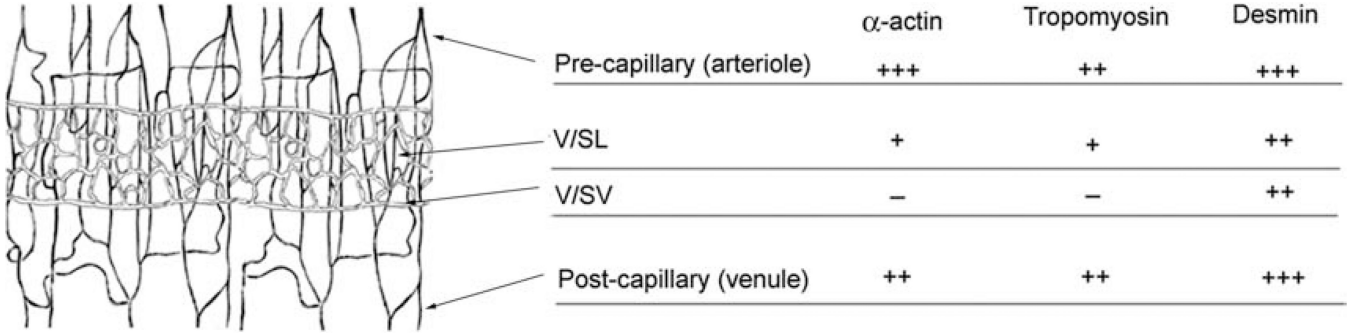

Figure 9.

Schematic drawing of the segment of the cochlear lateral-wall vessel, illustrating immunological heterogeneity of contractile protein expression in the different vessels. "–" = no expression of proteins (background level of fluorescent intensity); "+" = evidence of the presence of labeled proteins (a visually detectable level with low fluorescent intensity); "++" ~ "+++" = a Photoshop fluorescence intensity value greater than two or three times the "+" level, respectively.

Table 1

The Cochlear Pericyte Distribution in the V/SL and V/SV

Second Turn	V/SL (Precapillary)	V/SL (True Capillary)	V/SL (Postcapillary)	V/SV Capillary
Pericyte soma length	Range: 7.0–12.5 μm Mean ± SD: 9.0 ± 1.9 μm n = 50 cells	Range: 11.6–12.6 μm Mean ± SD: 11.6 ± 1.6 μm n = 50 cells	Range: 7.0–13.0 μm Mean ± SD: 9.7 ± 2.0 μm n = 50 cells	Range: 10.0–12.0 μm Mean ± SD: 10.9 ± 1.9 μm n = 50 cells
Distance between two neighbor PC somas	2.0–20 μm	Range: 50–87.5 μm Mean: 41 ± 23.0 μm n = 33 vessels	2.0–25 μm	Range: 50–100 μm Mean: 50 ± 18.5 μm n = 33 vessels
Ratio PC/EC		~1:1–1:2 Mean ± SD (0.76 ± 0.09)		~1:1–1:2 Mean ± SD (0.644 ± 0.08)

V/SL, vessels of the spiral ligament; V/SV, vessels of the stria vascularis; PC/EC, ratio of pericytes to endothelial cells; SD, standard deviation.